

# Comité de Suivi Individuel

## 2me année

Léo Boudet

Supervisor : Lucia DI CIACCIO (LAPP)  
CSI : Corinne GOY (LPSC), Diego GUADAGNOLI (LAPTh)  
Tutor : Frédérique MARION (LAPP)

6 septembre 2024



# Introduction

Search for new sources of CP violation with effective field theories in WZ diboson production with ATLAS

# Introduction

- Qualification as ATLAS author effective since 15th January.

V. Boisvert 98, P. Bokan 37, T. Bold 88a, M. Bomben 5, M. Bona 97, M. Boonekamp 139, A.G. Borbély 61, I.S. Bordulev 39, G. Borissov 94, D. Bortoletto 130, D. Boscherini 24b, M. Bosman 13, K. Bouaouda 36a, N. Bouchhar 168, L. Boudet 4, J. Boudreau 133, E.V. Bouhova-Thacker 94, D. Boumediene 42, R. Bouquet 59b,59a, A. Boveia 123, J. Boyd 37, D. Boye 30, I.R. Boyko 40, L. Bozianu 58, J. Bracinik 21, N. Brahimi 4, G. Brandt 176,

- Still involved in e/ $\gamma$  CP group ,  $\simeq 20\%$  working time.

# Contents

- 1 CP violation and EFT
- 2 Constraints on SMEFT via machine learning : design of BDTs
- 3 BDT optimisation
- 4 Conclusion and 2nd year summary

# CP violation and EFT

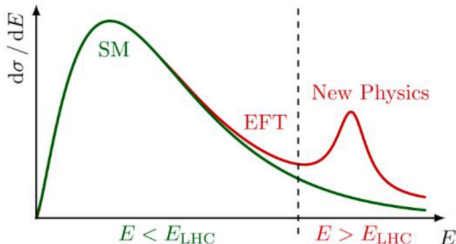
→ CP violation (CPV) : matter and antimatter interact differently

→ Necessary to explain matter excess in the Universe

→ Insufficient amount of CPV sources in Standard Model (SM)

→ Need for **indirect** search of new physics, possibly lying beyond energy reach of LHC

QUARKS		GAUGE BOSONS	
u	c	t	g
d	s	b	$\gamma$
e	$\mu$	$\tau$	Z
electron neutrino	muon neutrino	tau neutrino	W



# Standard Model Effective Field Theory (SMEFT)

- SM = **low energy** effective theory of a more complete model
- SM fields = relevant degrees of freedom at accessible energies

Let  $\Lambda$  be new physics energy scale,  $m_i$  SM particles masses :

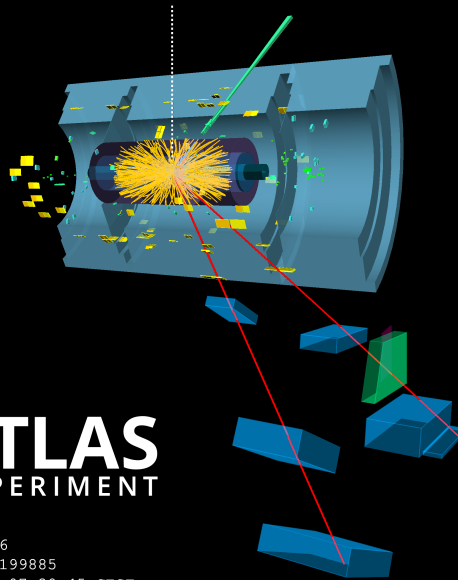
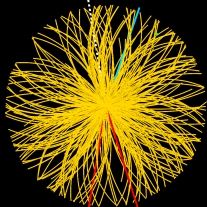
$$m_i \ll \sqrt{s} \ll \Lambda \quad (1)$$

The SMEFT Lagrangian is built adding operators of higher dimension in energy to the SM :

$$\mathcal{L}_{SMEFT} = \mathcal{L}_{SM} + \sum_{d>4} \sum_i \frac{c_{d,i}}{\Lambda^{d-4}} \mathcal{O}_{d,i} \quad (2)$$

- $\mathcal{O}_{d,i}$  contain **only SM fields**
- $c_{d,i}$  the **Wilson coefficients** → **parameters to constrain**

# Why the WZ process ?



Run: 302956

Event: 911199885

2016-06-29 07:39:45 CEST

# CPV with WZ diboson

Search for CPV via **anomalous triple gauge couplings (aTGC)** → Higgs sector and EW symmetry breaking

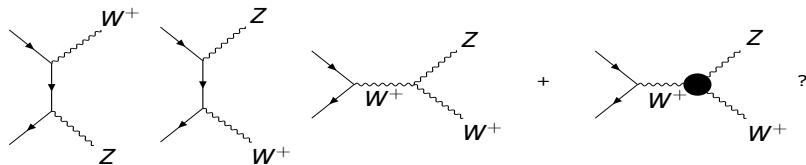


Figure – LO Feynman diagrams for  $W^+Z$  production with possible aTGC (black blob)

At LHC energy scale, the relevant dim 6 bosonic operators possibly providing a source of CPV are [1] :

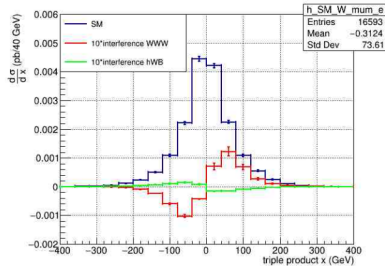
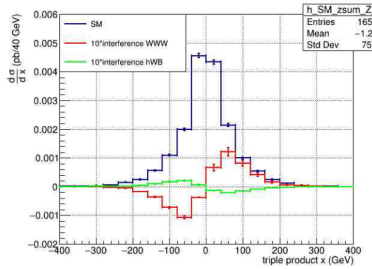
$$\mathcal{O}_{H\tilde{W}B} = \phi^\dagger \sigma_I \phi \tilde{W}^{I,\mu\nu} B_{\mu\nu} \quad \mathcal{O}_{\tilde{W}WW} = \varepsilon_{IJK} \tilde{W}_\nu^{I,\mu} W_\rho^{J,\nu} W_\mu^{K,\rho} \quad (3)$$

# CPV with WZ diboson

$$\sigma = \frac{1}{F} \int |\mathcal{M}|^2 d\text{ LIPS} \quad (F : \text{Moller's flux})$$

$$|\mathcal{M}|^2 = \left| \mathcal{M}_{SM} + \frac{1}{\Lambda^2} \mathcal{M}_6 \right|^2 = |\mathcal{M}_{SM}|^2 + \frac{2}{\Lambda^2} \Re(\mathcal{M}_{SM} \mathcal{M}_6^*) + \frac{1}{\Lambda^4} |\mathcal{M}_6|^2$$
$$|\mathcal{M}|^2 = SM + int.+quad.$$

CP-odd operators modify differential cross section  $d\sigma/dx$ , need to exploit new variables .



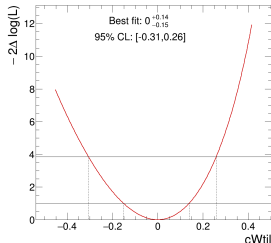
# Constraints on Wilson coefficients

- ① Select a CP-odd observable sensitive to  $\mathcal{O}_{H\tilde{W}B}$  ou  $\mathcal{O}_{\tilde{W}}$
- ② Likelihood fit on data with  $c_i$  as a free parameter

$$\mathcal{L}(c_i) = \frac{1}{\sqrt{(2\pi)^k |C|}} \exp\left(-\frac{1}{2}(\vec{x}_{data} - \vec{x}_{pred}(c_i))^T C^{-1} (\vec{x}_{data} - \vec{x}_{pred}(c_i))\right)$$

- $x_k$  the value in bin  $k$ ,  $C$  covariance matrix between bins
- data = ATLAS Run 2 data
- pred = SM + SM-EFT interference( $c_i$ ) + EFT quadratic ( $c_i^2$ )

- ③ Extract limits on coefficients  $c_{H\tilde{W}B}$  ou  $c_{\tilde{W}}$



$$-2\Delta\log \mathcal{L}(c_i) = -2\log\left(\frac{\mathcal{L}(c_i)}{\mathcal{L}(\hat{c}_i)}\right)$$

→ 68% and 95% confidence intervals

# Expected and observed existing ATLAS limits

Analyses of Vector Boson Fusion (VBF) processes also enable us to study aTGC :

Analyse	Observable	95% CI $c_{H\tilde{W}B}$	95% CI $c_{\tilde{W}}$
VBF $Z$ [2]	$\Delta\Phi_{jj}$	[-1.06, 1.06]	[-0.12, 0.12]
VBF $H \rightarrow W^*W$ [3]	$\Delta\Phi_{jj}$	[-1.2, 1.1] <sup>1</sup>	N/A
VBF $Z$ obs.	$\Delta\Phi_{jj}$	[0.23, 2.34]	[-0.11, 0.14]
VBF $H \rightarrow W^*W$ obs.	$\Delta\Phi_{jj}$	[-1.2, 1.1]	N/A
WZ (this work)	$p_\perp(\sum p^z, Z, W^{lep})$	[-3.97, 3.96]	[-0.21, 0.21]
WZ (this work)	$\varphi_W^*$	[-3.25, 3.19]	[-0.17, 0.17]
WZ (this work)	$\varphi_Z^*$	[-3.82, 3.74]	[-0.20, 0.21]

NB : Intervals in  $\text{TeV}^{-2}$ , describing limits expected from MC simulation and **limits observed**.

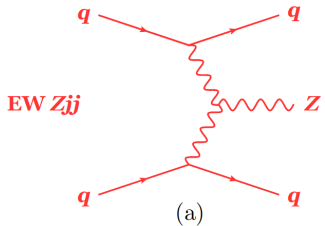
$$p_\perp(\sum p^z, Z, W^{lep}) = q_W(\sum_{lep} \vec{p^z}) \frac{\vec{p_Z} \times \vec{p_{W^{lep}}}}{|\vec{p_Z} \times \vec{p_{W^{lep}}}|}$$

$\varphi_V^*$  : decay lepton azimuthal angle around the axis defined by  $\vec{p}_V$

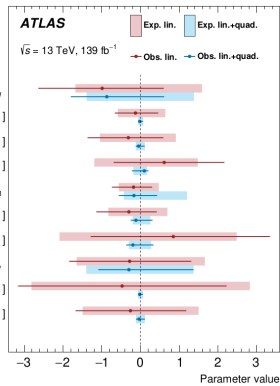
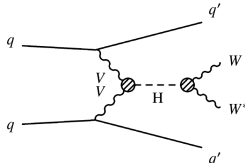
1. with quad term

# Int only vs int + quad

Zjj [2] 1 TGC : negligible



$H \rightarrow W^*W$  [3] 2 TGC : important

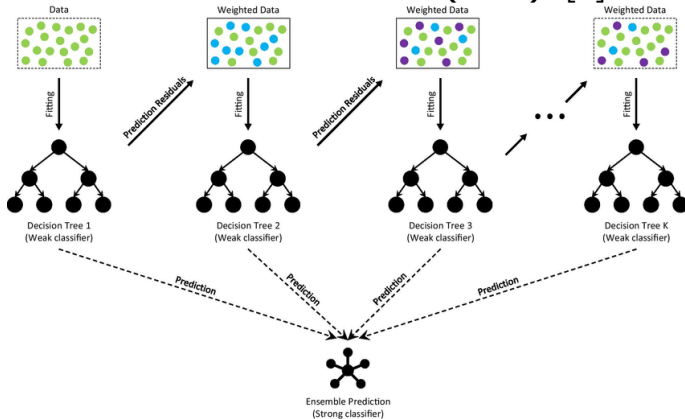


Wilson coefficient	Includes $ M_{d6} ^2$	95% confidence interval [ $\text{TeV}^{-2}$ ]		$p$ -value (SM)
		Expected	Observed	
$c_W/\Lambda^2$	no	[-0.30, 0.30]	[-0.19, 0.41]	45.9%
	yes	[-0.31, 0.29]	[-0.19, 0.41]	43.2%
$\tilde{c}_W/\Lambda^2$	no	[-0.12, 0.12]	[-0.11, 0.14]	82.0%
	yes	[-0.12, 0.12]	[-0.11, 0.14]	81.8%
$c_{HWB}/\Lambda^2$	no	[-2.45, 2.45]	[-3.78, 1.13]	29.0%
	yes	[-3.11, 2.10]	[-6.31, 1.01]	25.0%
$\tilde{c}_{HWB}/\Lambda^2$	no	[-1.06, 1.06]	[0.23, 2.34]	1.7%
	yes	[-1.06, 1.06]	[0.23, 2.35]	1.6%

# Constraints on SMEFT via machine learning

Unique observable → Multivariate analysis

## Gradient Boosted Decision Tree (BDTG) : [4]

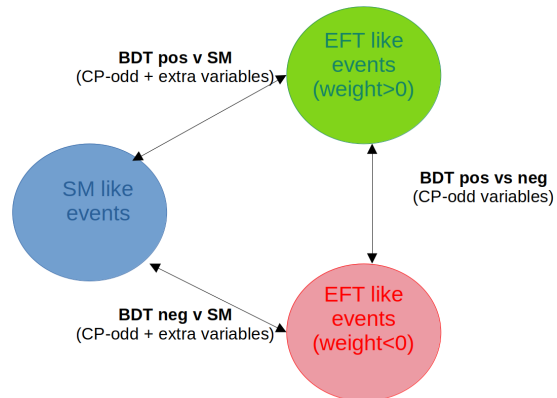


MC events  
splitted in 2  
sets :

- 1 Training
- 2 Testing

"Data" :  
simulated events  
used for training.

# Constraints on SMEFT via machine learning



Scores labelling :

- pos v SM :  $S_p$
- neg v SM :  $S_n$
- pos v neg :  $S_0$

Three distinct BDTs trained with TMVA :

**CP-odd variables :**

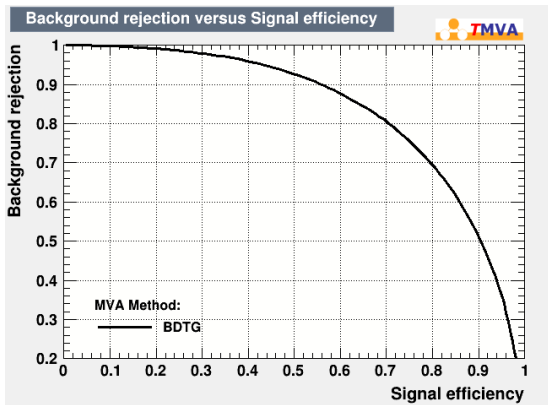
3 triple products,  $\sin \phi_{WZ}$ ,  
 $\varphi_W^*$ ,  $\varphi_Z^*$ ,  $\cos \theta_W^*$ ,  $\Delta\Phi(W^{lep}, Z)$

**Extra variables :**

$r_{21}$ ,  $p_T^Z$ ,  $p_T^{WZ}$ ,  $m_T^{WZ}$ ,  $m_T^W$ ,  
 $\Delta\Phi(W^{lep}, Z^{lep})$ ,  $E_T^{miss}$ ,  $p_{DNN}^{00}$ ,  
 $\cos \chi$

# BDT optimisation

A way to measure the performance of a BDT is with the Area Under the ROC Curve (AUC) :



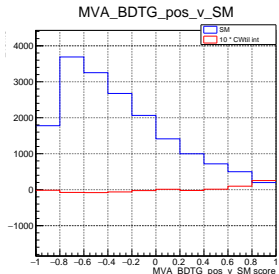
AUC maximisation for each BDT :

- ✓ selection of training variables
- ✓ choice of BDT hyperparameters
- ≈ k-folding training

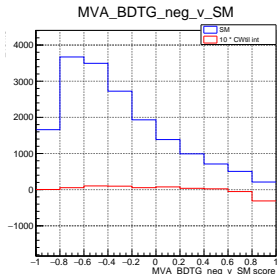
ROC curve BDT  $pos$  vs  $SM$  for  $\mathcal{O}_{\tilde{W}}$

# BDT scores combination

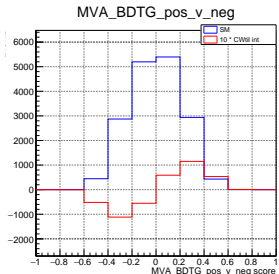
Score distributions for BDTs trained on  $\mathcal{O}_{\tilde{W}}$  EFT samples



$S_p$



$S_n$

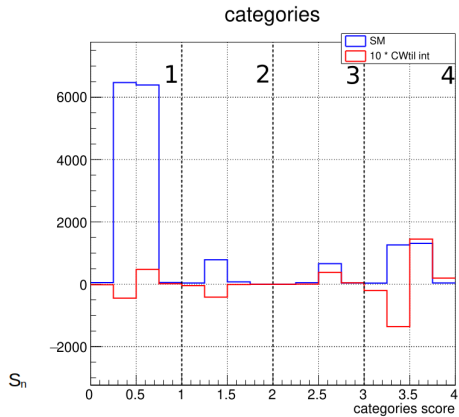
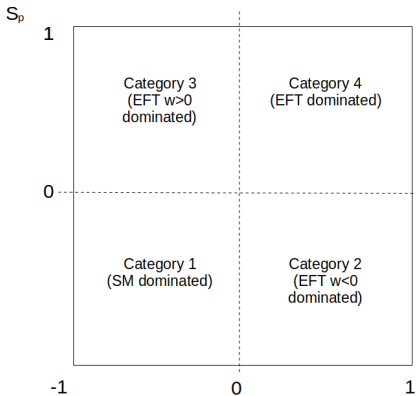


$S_0$

How to combine the three scores optimally?

# BDT scores combination

Similar behavior for both operators, EFT/SM ratio increased in category 4



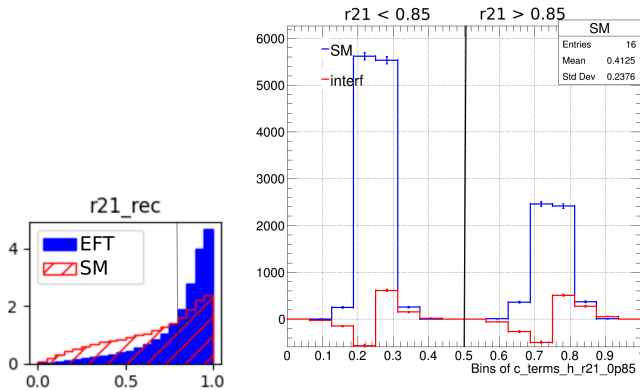
$$(\text{cat}(S_p, S_n) - 1) + S_0$$

# BDT scores combination

Amplification of  $S_0$  distribution shape :

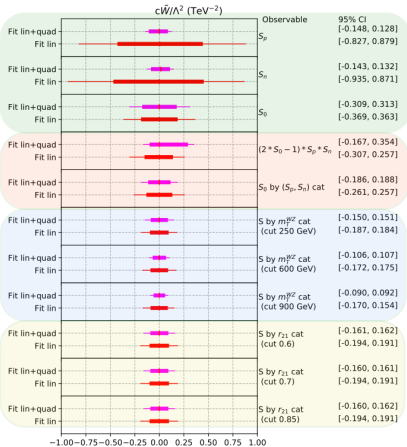
$$S = S_0 \times \frac{S_p + 1}{2} \times \frac{S_n + 1}{2}$$

Splitting S by categories, e.g.  $r_{21} = \frac{p_T^{V2}}{p_T^{V1}}$  (cut 0.85)

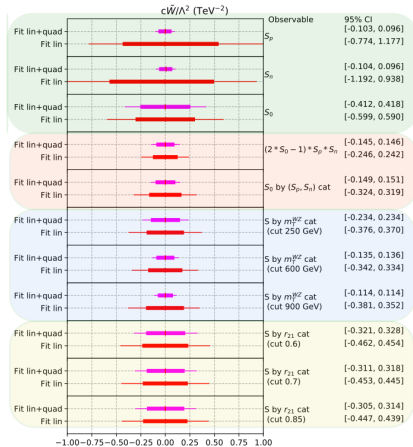


# Results summary : $c_{\tilde{W}}$ limits

TMVA



XGBoost



Single BDT score, basic combinations, combinations by  $m_T^{WZ}$  category and by  $r_{21}$  category

# Conclusion

Fits results (lin+quad) :

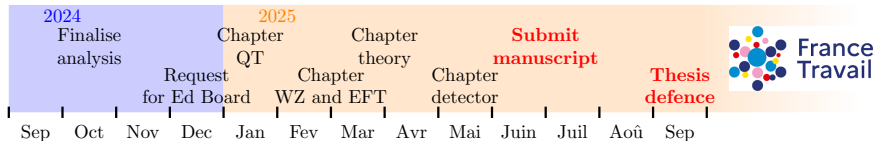
Analyse	Observable	95% CI $c_{H\tilde{W}B}$	95% CI $c_{\tilde{W}}$
VBF $Z$ [2]	$\Delta\Phi_{jj}$	[-1.06, 1.06]	[-0.12, 0.12]
VBF $H \rightarrow W^*W$ [3]	$\Delta\Phi_{jj}$	[-1.2, 1.1]	N/A
WZ (this work)	$p_\perp(\sum p^z, Z, W^{lep})$	[-3.97, 3.96]	[-0.21, 0.21]
WZ (this work)	$\varphi_W^*$	[-3.25, 3.19]	[-0.17, 0.17]
WZ (this work)	$\varphi_Z^*$	[-3.82, 3.74]	[-0.20, 0.21]
WZ (this work)	$S(m_T^{WZ})$ , cut 600 GeV	[-1.78, 1.75]	[-0.11, 0.11]
WZ (this work)	$S(m_T^{WZ})$ , cut 900 GeV	[-1.77, 1.80]	[-0.09, 0.09]
WZ (this work)	$S_0(S_p, S_n)$	[-1.88, 1.91]	[-0.19, 0.19]

- Shrinks CI widths up by more than a factor 2
- Competitive expected limits for  $\mathcal{O}_{\tilde{W}}$
- Have not reached same sensitivity for  $\mathcal{O}_{H\tilde{W}B}$

# To-do list 3rd year

- k-folding training to take advantage of the full statistics
- Implement trained BDTs in LAPPVVAnalyses framework
- Apply to Run 2 data, proceed to unfolding
- ... manuscript writing

# To-do list 3rd year



Manuscript content as planned to this day :

- ① The Standard Model and the EW symmetry breaking
- ② The LHC and the ATLAS detector
- ③ Low  $p_T$  electron identification in ATLAS
- ④ Mesurement of WZ cross sections
- ⑤ Constraints on SMEFT CP-odd operators

Possible splitting of chapters.

# Perspectives 3rd year

- Publication of WZ analysis end of autumn/winter
- Talk to Multiboson Interaction workshop in Toulouse (25th-27th Sep) : overview of SMEFT CPV studies in ATLAS



- Talk to the physics department of Jagiellonian University of Krakow (week of 7th Oct)

# Thank you for listening!

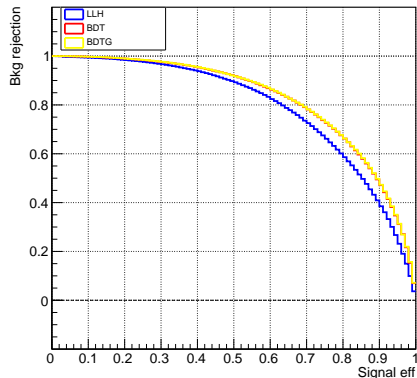
- [1] Céline Degrande et Julien Touchèque. “A Reduced basis for CP violation in SMEFT at colliders and its application to Diboson production”. In : *J. High Energ. Phys.* 2022.4 (avr. 2022). arXiv :2110.02993 [hep-ph], p. 32.
- [2] Collaboration ATLAS. “Differential cross-section measurements for the electroweak production of dijets in association with a Z boson in proton–proton collisions at ATLAS”. In : *The European physical journal. C* 81.2 (2021), p. 163.
- [3] Atlas Collaboration et al. “Integrated and differential fiducial cross-section measurements for the vector boson fusion production of the Higgs boson in the  $H \rightarrow WW \rightarrow e\nu\mu\nu$  decay channel at 13 TeV with the ATLAS detector”. In : *Physical Review D* 108.7 (2023), p. 072003.
- [4] Haowen Deng et al. “Ensemble learning for the early prediction of neonatal jaundice with genetic features”. In : *BMC medical informatics and decision making* 21 (2021), p. 1-11.

# Back-up

# BDT types

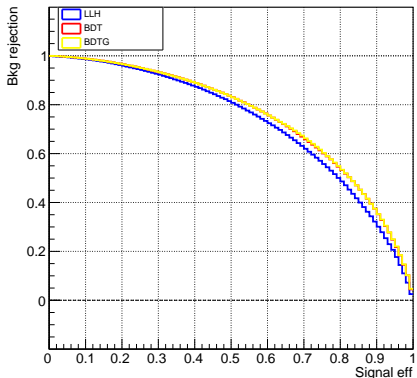
$\mathcal{O}_{\tilde{W}}$  (pos vs SM)

MVA\_Likelihood



$\mathcal{O}_{H\tilde{W}B}$  (pos vs SM)

MVA\_Likelihood



# List of dim 6 operators

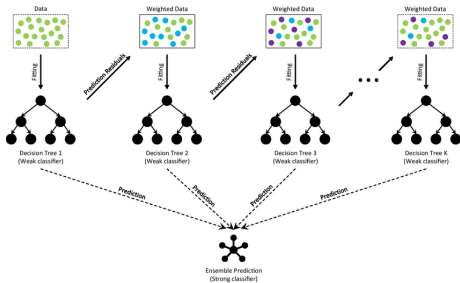
$U(3)^5$  flavour symmetry : all generations affected by the same effects

$\mathcal{L}_6^{(1)} - X^3$		$\mathcal{L}_6^{(6)} - \psi^2 X H$		$\mathcal{L}_6^{(8b)} - (\bar{R}R)(\bar{R}R)$	
$Q_G$	$f^{abc} G_{\mu}^{ab} G_{\nu}^{bc} G_{\rho}^{ca}$	$Q_{eW}$	$(\bar{l}_p \sigma^{\mu\nu} e_r) \sigma^i H W_{\mu\nu}^i$	$Q_{ee}$	$(\bar{e}_p \gamma_i e_r) (\bar{e}_s \gamma^\mu e_t)$
$Q_{\tilde{G}}$	$f^{abc} \tilde{G}_{\mu}^{ab} G_{\nu}^{bc} G_{\rho}^{ca}$	$Q_{eB}$	$(\bar{l}_p \sigma^{\mu\nu} e_r) H B_{\mu\nu}$	$Q_{eu}$	$(\bar{u}_p \gamma_\mu u_r) (\bar{u}_s \gamma^\mu u_t)$
$Q_W$	$\varepsilon^{ijk} W_{\mu}^{i\nu} W_{\nu}^{j\rho} W_{\rho}^{k\mu}$	$Q_{uG}$	$(\bar{q}_p \sigma^{\mu\nu} T^a u_r) \bar{H} G_{\mu\nu}^a$	$Q_{sd}$	$(\bar{d}_p \gamma_\mu d_r) (\bar{d}_s \gamma^\mu d_t)$
$Q_{\tilde{W}}$	$\varepsilon^{ijk} \tilde{W}_{\mu}^{i\nu} W_{\nu}^{j\rho} W_{\rho}^{k\mu}$	$Q_{uW}$	$(\bar{q}_p \sigma^{\mu\nu} u_r) \sigma^i \bar{H} W_{\mu\nu}^i$	$Q_{cu}$	$(\bar{e}_p \gamma_\mu e_r) (\bar{u}_s \gamma^\mu u_t)$
$\mathcal{L}_6^{(2)} - H^6$		$\mathcal{L}_6^{(1)} - H^4 D^2$		$\mathcal{L}_{ud}^{(1)} - (\bar{u}_p \sigma^{\mu\nu} d_r) \bar{H} B_{\mu\nu}$	
$Q_H$	$(H^\dagger H)^3$	$Q_{uG}$	$(\bar{q}_p \sigma^{\mu\nu} T^a d_r) H G_{\mu\nu}^a$	$Q_{ud}^{(1)}$	$(\bar{u}_p \gamma_\mu u_r) (\bar{d}_s \gamma^\mu d_t)$
		$Q_{uW}$	$(\bar{q}_p \sigma^{\mu\nu} d_r) \sigma^i H W_{\mu\nu}^i$	$Q_{ud}^{(8)}$	$(\bar{u}_p \gamma_\mu T^a u_r) (\bar{d}_s \gamma^\mu T^a d_t)$
$Q_{HD}$	$(H^\dagger H) \square (H^\dagger H)$	$Q_{dB}$	$(\bar{q}_p \sigma^{\mu\nu} d_r) H B_{\mu\nu}$		
$\mathcal{L}_6^{(4)} - X^2 H^2$		$\mathcal{L}_6^{(7)} - \psi^2 H^2 D$		$\mathcal{L}_6^{(8c)} - (\bar{L}\bar{L})(\bar{R}R)$	
$Q_{HG}$	$H^\dagger H G_{\mu\nu}^a G^{a\mu\nu}$	$Q_{HI}^{(1)}$	$(H^\dagger i \frac{\overleftrightarrow{D}}{\mu} H) (\bar{l}_p \gamma^\mu l_r)$	$Q_{le}$	$(\bar{l}_p \gamma_\mu l_r) (\bar{e}_s \gamma^\mu e_t)$
$Q_{H\tilde{G}}$	$H^\dagger H \tilde{G}_{\mu\nu}^a G^{a\mu\nu}$	$Q_{HI}^{(3)}$	$(H^\dagger i \frac{\overleftrightarrow{D}}{\mu} H) (\bar{l}_p \sigma^i \gamma^\mu l_r)$	$Q_{lu}$	$(\bar{l}_p \gamma_\mu l_r) (\bar{u}_s \gamma^\mu u_t)$
$Q_{HW}$	$H^\dagger H W_{\mu\nu}^a W^{a\mu\nu}$	$Q_{He}$	$(H^\dagger i \frac{\overleftrightarrow{D}}{\mu} H) (\bar{e}_p \gamma^\mu e_r)$	$Q_{ld}$	$(\bar{l}_p \gamma_\mu l_r) (\bar{d}_s \gamma^\mu d_t)$
$Q_{H\tilde{W}}$	$H^\dagger H \tilde{W}_{\mu\nu}^a W^{a\mu\nu}$	$Q_{Hq}^{(1)}$	$(H^\dagger i \frac{\overleftrightarrow{D}}{\mu} H) (\bar{q}_p \gamma^\mu q_r)$	$Q_{qe}$	$(\bar{q}_p \gamma_\mu q_r) (\bar{e}_s \gamma^\mu e_t)$
$Q_{HB}$	$H^\dagger H B_{\mu\nu} B^{\mu\nu}$	$Q_{Hq}^{(3)}$	$(H^\dagger i \frac{\overleftrightarrow{D}}{\mu} H) (\bar{q}_p \sigma^{i\mu} \gamma^\mu q_r)$	$Q_{qv}^{(1)}$	$(\bar{q}_p \gamma_\mu q_r) (\bar{u}_s \gamma^\mu u_t)$
$Q_{H\tilde{B}}$	$H^\dagger H \tilde{B}_{\mu\nu} B^{\mu\nu}$	$Q_{Hu}$	$(H^\dagger i \frac{\overleftrightarrow{D}}{\mu} H) (\bar{u}_p \gamma^\mu u_r)$	$Q_{qv}^{(8)}$	$(\bar{q}_p \gamma_\mu T^a q_r) (\bar{u}_s \gamma^\mu T^a u_t)$
$Q_{H\tilde{W}B}$	$H^\dagger \sigma^i H W_{\mu\nu}^i B^{\mu\nu}$	$Q_{Hd}$	$(H^\dagger i \frac{\overleftrightarrow{D}}{\mu} H) (\bar{d}_p \gamma^\mu d_r)$	$Q_{qd}^{(1)}$	$(\bar{q}_p \gamma_\mu q_r) (\bar{d}_s \gamma^\mu d_t)$
$Q_{H\tilde{W}B}$	$H^\dagger \sigma^i H \tilde{W}_{\mu\nu}^i B^{\mu\nu}$	$Q_{Hud} + \text{h.c.}$	$i(\bar{H}^\dagger D_\mu H) (\bar{u}_p \gamma^\mu d_r)$	$Q_{qd}^{(8)}$	$(\bar{q}_p \gamma_\mu T^a q_r) (\bar{d}_s \gamma^\mu T^a d_t)$
$\mathcal{L}_6^{(5)} - \psi^2 H^3$		$\mathcal{L}_6^{(8a)} - (LL)(LL)$		$\mathcal{L}_6^{(8d)} - (LR)(RL), (LR)(LR)$	
$Q_{eH}$	$(H^\dagger H) (\bar{l}_p e_r, H)$	$Q_{ll}$	$(\bar{l}_p \gamma_\mu l_r) (\bar{l}_s \gamma^\mu l_t)$	$Q_{ledq}$	$(\bar{l}_p e_r) (\bar{d}_s q_{tj})$
$Q_{uH}$	$(H^\dagger H) (\bar{q}_p u_r, \bar{H})$	$Q_{qq}^{(1)}$	$(\bar{q}_p \gamma_\mu q_r) (\bar{q}_s \gamma^\mu q_t)$	$Q_{qvqd}^{(1)}$	$(\bar{q}_p^a u_s) e_{jk} (\bar{q}_s^b d_t)$
$Q_{dH}$	$(H^\dagger H) (\bar{q}_p d_r, H)$	$Q_{qq}^{(3)}$	$(\bar{q}_p \gamma_\mu q^a r) (\bar{q}_s \gamma^\mu \sigma^a q_t)$	$Q_{qvqd}^{(8)}$	$(\bar{q}_p^a T^a u_s) e_{jk} (\bar{q}_s^b T^a d_t)$
		$Q_{lq}^{(1)}$	$(\bar{l}_p \gamma_\mu l_r) (\bar{q}_s \gamma^\mu q_t)$	$Q_{lqqn}^{(1)}$	$(\bar{l}_p e_r) e_{jk} (\bar{q}_s^a u_t)$
		$Q_{lq}^{(3)}$	$(\bar{l}_p \gamma_\mu \sigma^i l_r) (\bar{q}_s \gamma^\mu \sigma^i q_t)$	$Q_{lqqn}^{(3)}$	$(\bar{l}_p^a \sigma_{\mu\nu} e_r) \varepsilon_{jk} (\bar{q}_s^a \sigma^{\mu\nu} u_t)$

- **Bosonic**
- **Boson-fermion**
- **4-fermion**

# BDTG hyperparameters

- Number of trees
- Tree maximal depth
- Minimal Node Size
- Shrinkage ( $\simeq$  learning rate) :  
maximal impact of a BDT on  
the final model



# Variable ranking $S_0$ for $\mathcal{O}_{H\tilde{W}B}$

Variable	AUC(N-1)	Importance (%)	AUC(N-1) - AUC(N)
phiStarW_rec	0.6305	0.1734	0.0099
TP_WZLepmWLep_rec	0.6352	0.0917	0.0052
phiStarZ_rec	0.6361	0.0765	0.0044
cosThetaStarZ_rec	0.6367	0.0665	0.0038
TP_WZLeppWLep_rec	0.6368	0.0646	0.0037
cosThetaStarW_rec	0.6371	0.0585	0.0033
sinPhiWZ_rec	0.6375	0.0515	0.0029
TP_zZWLep_rec	0.6375	0.0514	0.0029
dPhiWIz_rec	0.6387	0.0303	0.0017

# Variable ranking $S_0$ for $\mathcal{O}_{\tilde{W}}$

Variable	AUC(N-1)	Importance (%)	AUC(N-1) - AUC(N)
phiStarZ_rec	0.6257	0.3538	0.0204
cosThetaStarZ_rec	0.6410	0.0885	0.0051
phiStarW_rec	0.6413	0.0830	0.0048
sinPhiWZ_rec	0.6425	0.0617	0.0036
TP_WZLeppWLep_rec	0.6426	0.0613	0.0035
TP_WZLepmWLep_rec	0.6428	0.0565	0.0033
TP_zZWLepl_rec	0.6450	0.0187	0.0011
dPhiWIz_rec	0.6451	0.0177	0.0010
cosThetaStarW_rec	0.6451	0.0172	0.0010

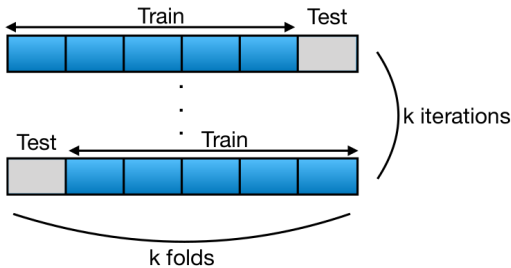
# Variable ranking $S_n$ for $\mathcal{O}_{\tilde{W}}$

Variable	AUC(N-1)	Importance (%)	AUC(N-1) - AUC(N)
r21_rec	0.8018	0.1891	2.8166
p0ODNN_rec	0.8261	0.0254	0.3777
pTWZ_rec	0.8266	0.0223	0.3329
mTWZ_rec	0.8273	0.0177	0.2638
phiStarZ_rec	0.8287	0.0081	0.1200
cosThetaStarW_rec	0.8292	0.0050	0.0740
pTZ_rec	0.8292	0.0049	0.0724
cosThetaStarZ_rec	0.8295	0.0030	0.0452
DphiWIIZlss_rec	0.8295	0.0028	0.0420
sinPhiWZ_rec	0.8297	0.0017	0.0257
phiStarW_rec	0.8297	0.0015	0.0228
dPhiWIIZ_rec	0.8297	0.0015	0.0218
TP_WZLeppWLep_rec	0.8298	0.0011	0.0158
mTW_rec	0.8299	0.0004	0.0060
TP_WZLepmWLep_rec	0.8299	0.0004	0.0056
MET	0.8299	0.0002	0.0029
TP_zZWLepl_rec	0.8300	0.0008	0.0124
cosChi_WZRef_rec	0.8300	0.0009	0.0127

# Variable ranking $S_p$ for $\mathcal{O}_{\tilde{W}}$

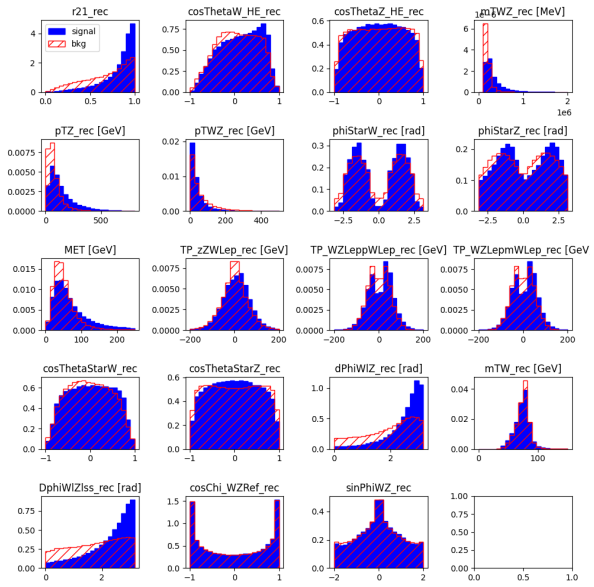
Variable	AUC(N-1)	Importance (%)	AUC(N-1) - AUC(N)
r21_rec	0.8018	0.1975	0.0295
pTWZ_rec	0.8266	0.0310	0.0046
p0ODNN_rec	0.8272	0.0272	0.0041
mTWZ_rec	0.8283	0.0197	0.0029
phiStarZ_rec	0.8299	0.0089	0.0013
pTZ_rec	0.8301	0.0075	0.0011
DphiWIZlss_rec	0.8304	0.0055	0.0008
cosThetaStarW_rec	0.8305	0.0048	0.0007
dPhiWIZ_rec	0.8306	0.0046	0.0007
cosThetaStarZ_rec	0.8307	0.0035	0.0005
TP_WZLeppWLep_rec	0.8309	0.0022	0.0003
phiStarW_rec	0.8310	0.0019	0.0003
cosChi_WZRef_rec	0.8310	0.0018	0.0003
TP_WZLepmWLep_rec	0.8310	0.0015	0.0002
MET	0.8311	0.0012	0.0002
mTW_rec	0.8311	0.0012	0.0002
sinPhiWZ_rec	0.8312	0.0006	0.0001
TP_zZWLepl_rec	0.8313	0.0001	0.0000

# k-folding



Resulting in  $k$  separate BDTs.

# Input variables : $S_p$ for $\mathcal{O}_{\tilde{W}}$

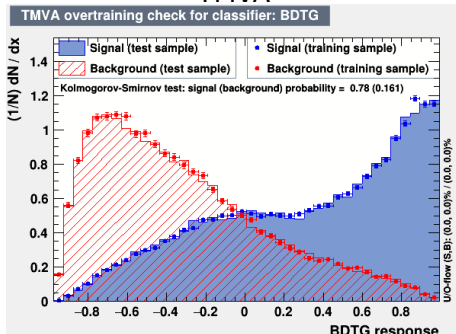


# Comparison TMVA vs XGBoost

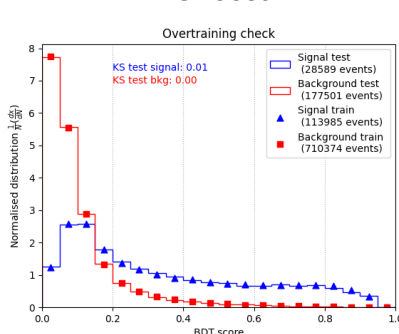
While being designed differently, XGBoost serves the same purpose as TMVA.

- worse signal (=EFT) acceptance
- better background (=SM) rejection

TMVA



XGBoost



Example :  $S_p$  score for  $c_{\tilde{W}}$ , comparable AUC (0.83 vs 0.83)

# Results summary

## Fit on $\mathcal{O}_{\tilde{W}}$

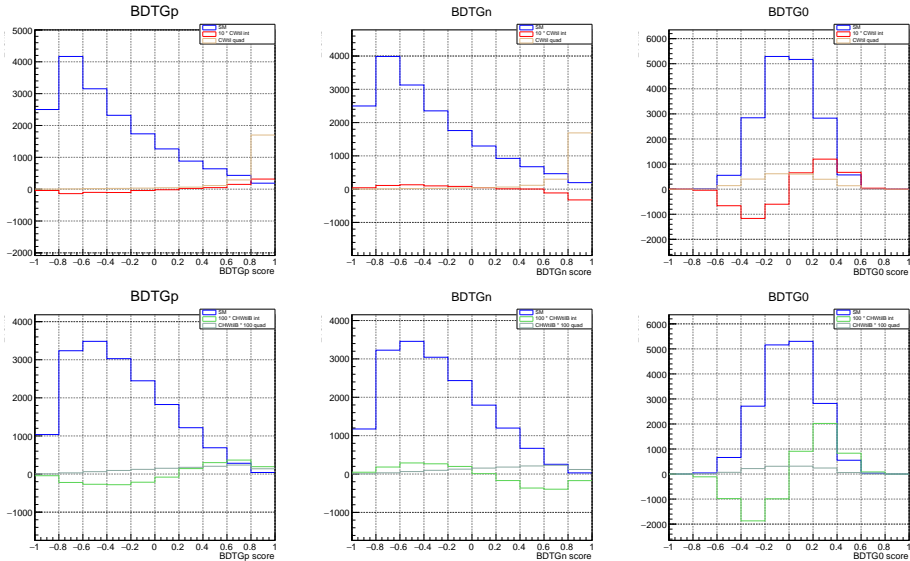
	Best observable	95% CI lin	95% CI lin+quad
TMVA	$S(m_T^{WZ})$ , cut 900 GeV	[-0.17, 015]	[-0.09, 0.09]
XGBoost	$S(m_T^{WZ})$ , cut 900 GeV	[-0.38, 035]	[-0.11, 0.11]

## Fit on $\mathcal{O}_{H\tilde{W}B}$

	Best observable	95% CI lin	95% CI lin+quad
TMVA	$S(m_T^{WZ})$ , cut 600 GeV	[-1.84, 1.81]	[-1.77, 1.80]
XGBoost	$S_0(S_p, S_n)$	[-1.83, 1.15]	[-1.68, 1.07]

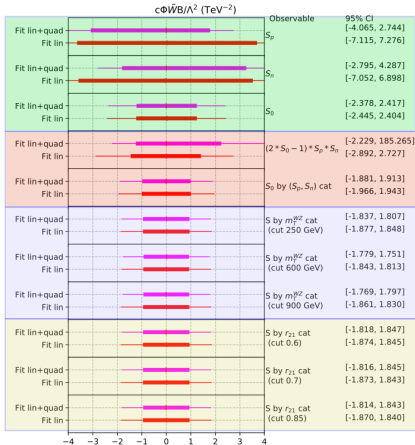
# Impact of quadratic term

## BDT scores distributions :

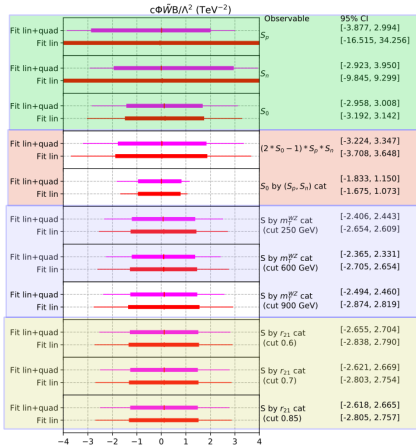


# Results summary : $c_{H\tilde{W}B}$ limits

TMVA



XGBoost



Single BDT score, basic combinations, combinations by  $m_T^{WZ}$  category and by  $r_{21}$  category

# Presentations

**ATLAS week (12th-16th Feb)**  
Poster presented on QT results



# Presentations

**e/ $\gamma$  workshop (8th-12th Apr)**  
Presentation on all of the electron  
ID subgroup results with release  
22



# Presentations

## ICHEP (18th-24th Jul)

Poster presented at ICHEP on behalf of  $e/\gamma$  for final Run2 performances plots :

### Final Performances for electron and photon calibration, reconstruction and identification with the ATLAS detector



Léo Boudet, on behalf of the ATLAS collaboration

Les Amis de l'ATLAS - Laboratoire d'Annecy de Physique des Particules (LAPP)

#### Chapters

All the LHC electrons and photons play a crucial role for precision measurements of the Higgs boson properties as well as Standard Model parameters such as the weak mixing angle or the W boson mass. In addition, they are crucial for searches such as Dark Matter production or Beyond Standard Model physics. This poster presents the final Run2 performances of the electron and photon reconstruction and identification, with a good understanding of the detector performance in order to keep under control the systematic uncertainties arising from electron and photon detection.

After triggering, prompt electron and photon detection goes through three steps: **reconstruction** → **energy calibration** → **identification**.

**Object reconstruction**:  
Each event contains an object digitized after energy loss in the electromagnetic calorimeter through electromagnetic showering, leaving energy clusters. These clusters are then reconstructed into tracks. These tracks are then matched with the main detector tracks. Charge and momentum are then calculated for each electron or converted photon (imposing no constraint on the track), while those not matched are re-evaluated using reconstructed photon candidates.

**Energy calibration**:  
To facilitate the energy assignment of electrons and photons, the successive steps are:

- estimation of the energy loss from the energy deposited in the calorimeter using a simulation-based ESD regression algorithm;
- adjustment of the relative energy scale for each electron or photon candidate;
- correction for residual noise fluctuations in the energy scale using a linear fit to the energy loss and adjustment of the overall energy scales ( $\alpha$ ) and resolutions ( $\sigma$ ) in data sets  $E_T$  vs  $\tau$  samples

where  $\alpha = \alpha(E_T) + \alpha(\eta)$  and  $\sigma = \sigma(E_T) \oplus \sigma(\eta)$ .  
Ultimately, the calibrated energy measurements achieve a resolution of about 3% [1] for

- = 0.6% (resp. 0.2%) for electron  $p_T > 10$  GeV (resp. 1 GeV);
- = 0.2% for photons of  $E_T > 10$  GeV

These improvements are validated using independent event samples.

**Electron identification**:  
Identification (ID) aims to discriminate electrons originating from the hadronic source from those originating from the lepton source (e.g. Z boson decay). Depending on the  $p_T$ , several methods are used to measure ID efficiency [2]:

- for  $p_T < 10$  GeV: a two-dimensional cut on  $E_T$  and  $\eta$  for  $p_T$  down to 0.5 GeV and up to 20 GeV;
- for  $p_T > 10$  GeV: an increased mass estimator for  $p_T$  from 15 to 200 GeV;
- for  $p_T > 200$  GeV: a deep learning relative isolation method.

Methods are later combined to perform 2D likelihood based working points [3].

**Photon identification**:  
Two main types of photons can be distinguished for identification purposes: unconverted and converted photons. The methods are described below:

- (1) radiative  $E_T$  ( $E_T = E_T^{\text{jet}} + \epsilon$ ):  
These methods are used and combined:
  - (1) radiative  $E_T = E_T^{\text{jet}} + \epsilon$  down to  $E_T = 10$  GeV;
  - (2) extrapolation from electron ID measurement ( $E_T = E_T^{\text{jet}} + \epsilon$ ) for same  $E_T$  range by transforming cluster shape and position using a method based on  $E_T$  ratio and isolation differences between prompt and background photons [2];
- (2) photon conversion:  
These methods are used and combined:
  - (1) radiative  $E_T = E_T^{\text{jet}} + \epsilon$  down to  $E_T = 10$  GeV;
  - (2) extrapolation from electron ID measurement ( $E_T = E_T^{\text{jet}} + \epsilon$ ) for same  $E_T$  range by transforming cluster shape and position using a method based on  $E_T$  ratio and isolation differences between prompt and background photons [2];



#### References



# ADUM formations

Total : 203 hours

Formation	Catégorie	Heures
Exercer son esprit critique : données et raisonnner	Transversale	20
Théorie des groupes	Scientifique	18
European school of high energy physics du CERN	Scientifique	40
Summer school 'Methods of Effective Field Theor	Scientifique	40
Cours d'espagnol à l'Université Savoie Mont-Blanc	Transversale	12
Encadrer efficacement des TD-22-2	Professionnelle	7
Enseignement à l'Université Savoie Mont-Blanc (2	Professionnelle	8
RÉDIGER VOS ARTICLES ET VOTRE THÈSE AVEC	Scientifique	10
Cours d'espagnol à l'Université Savoie Mont-Blanc	Transversale	6
MOOC Ethique de la recherche	Transversale	15
MOOC Doctorat et poursuite de carrière	Professionnelle	24
Enseignement à l'Université Savoie Mont-Blanc (2	Professionnelle	3

## Répartition des heures

